







## A severe landslide event in the Alpine foreland under possible future climate and land-use changes

Douglas Maraun <sup>1✉</sup>, Raphael Knevels <sup>2</sup>, Aditya N. Mishra<sup>1,3</sup>, Heimo Truhetz <sup>1</sup>, Emanuele Bevacqua <sup>1,4,5</sup>, Herwig Proske<sup>6</sup>, Giuseppe Zappa <sup>7</sup>, Alexander Brenning<sup>2</sup>, Helene Petschko <sup>2</sup>, Armin Schaffer<sup>1</sup>, Philip Leopold<sup>8</sup> & Bryony L. Puxley<sup>4</sup>

Landslides are a major natural hazard, but uncertainties about their occurrence in a warmer climate are substantial. The relative role of rainfall, soil moisture, and land-use changes and the importance of climate change mitigation are not well understood. Here, we develop an event storyline approach to address these issues, considering an observed event in Austria with some 3000 landslides as a showcase. We simulate the event using a convection permitting regional climate model and a statistical landslide model at present and a range of plausible future climate and land use conditions. Depending on the changes of rainfall and soil moisture, the area affected during a 2009-type event could grow by 45% at 4 K global warming, although a slight reduction is also possible. Such growth could be reduced to less than 10% by limiting global warming according to the Paris agreement. Anticipated land-use changes towards a climate-resilient forest would fully compensate for such a limited increase in hazard.

<sup>1</sup>Wegener Center for Climate and Global Change, University of Graz, Graz, Austria. <sup>2</sup>Friedrich Schiller University Jena, Department of Geography, Jena, Germany. <sup>3</sup>FWF-DK Climate Change, University of Graz, Graz, Austria. <sup>4</sup>Department of Meteorology, University of Reading, Reading, UK. <sup>5</sup>Helmholtz Centre for Environmental Research—UFZ, Leipzig, Germany. <sup>6</sup>Joanneum Research, Remote Sensing and Geoinformation Department, Graz, Austria. <sup>7</sup>National Research Council of Italy, Institute of Atmospheric Sciences and Climate, Bologna, Italy. <sup>8</sup>AIT Austrian Institute of Technology GmbH, Vienna, Austria. ✉email: [douglas.maraun@uni-graz.at](mailto:douglas.maraun@uni-graz.at)

Landslides are a major natural hazard and an important threat to population, urban settlements, infrastructure and environment across the Alps and their forelands<sup>1</sup>. The susceptibility of a location to landslides depends strongly on the geological conditions, the topography and the vegetation<sup>2–4</sup>. In the Alps, landslides are mainly triggered by heavy rainfall or rapid snow melt<sup>5</sup>. The interplay of these triggering factors with preconditioning from high soil moisture<sup>6–8</sup> makes landslide a compound event<sup>9</sup>.

A particularly extreme event happened during June 22–26 2009<sup>10</sup> when a persistent cut-off low over the Adriatic (Fig. 1a) brought warm and moist air to Austria, causing three days of heavy rainfall in northern and eastern Austria<sup>11</sup>. In the Feldbach district, in the South–Eastern Alpine forelands, the heavy rain associated with thunderstorms triggered more than 3000 landslides during that event (Fig. 1b; the area marked by the black rectangle is referred to as Feldbach region in the following). High soil moisture, caused by a high snow depth during the preceding winter<sup>10</sup>, may have contributed to the severity of the event. A state of emergency was issued for the whole Feldbach district, and several houses had to be evacuated. From about 1700 private damage claims submitted to the state government, 560 were from the district. The cost for the state of Styria of the actual disaster operation and reconstruction surpassed 13.4 million euros<sup>10</sup>, not including damages paid privately or by insurance companies. Anthropogenic factors played an important role in the severity of the 2009 event, as many of the observed landslides were associated with steep or unsecured embankments, filling of slopes or paved areas<sup>10</sup>.

Climate change will almost certainly affect the preconditioning and triggering of landslides: total winter, but also spring, precipitation is projected to increase over the Alps<sup>12,13</sup>. The character of extreme rainfall is expected to change as well: in response to an increasing water holding capacity of the atmosphere and to changes in the large-scale atmospheric circulation and stability<sup>14</sup>. Over the Alps, heavy summertime rainfall is projected to increase, albeit with substantial uncertainties<sup>13,15,16</sup>. In the eastern Alpine forelands, spells of summertime extreme rainfall typically occur along with cut-off lows as well as Vb cyclones and Genoa lows<sup>17,18</sup>. The rainfall associated with such storms may increase in a warmer climate<sup>19–21</sup>. In contrast, the preconditioning soil moisture content is projected to decrease over Europe<sup>22</sup>, consistent with a higher potential for evapotranspiration<sup>23</sup> and a reduced snowcover<sup>13,24</sup>. Given these projected changes in

landslide drivers, it is conceivable that also the landslide hazard may change in a warmer climate<sup>6,7</sup>. Climate change is just one possible driver of changes in landslide hazards. Also, changes in land use and land cover (LULC) modulate the effect of changes in rainfall and soil moisture<sup>7,25,26</sup>. In particular changes in forest cover may be relevant for landslide occurrence, as the root systems of trees stabilise the soil<sup>27</sup>. The relative importance of changes in these hazard drivers has not yet been investigated.

Despite the growing number of studies on the influence of climate change on landslide hazard<sup>28–35</sup>, there is still substantial uncertainty about the identified changes: individual studies project different, even opposite, changes in the occurrence of landslides. Part of these differences may be explained by the different climatic and geological conditions across the regions considered for the analyses. But crucially, the results also depend on the chosen approach. In particular, several of these studies did not consider the effect of changes in soil moisture, thus introducing a substantial source of uncertainty. Moreover, many studies did not account for uncertainties in climate projections, thus being very sensitive to the chosen climate model.

Furthermore, to our knowledge, all studies based on climate modelling suffer from common modelling limitations. Importantly, none of these studies used convection permitting climate models with a resolution high enough to realistically simulate localised intense summertime rain showers<sup>36</sup> and to plausibly represent changes in such events<sup>37</sup>. Furthermore, global climate models (GCMs) typically suffer from large-scale circulation biases, which distort the simulated local weather conditions, but often cannot be overcome by downscaling or bias adjustment<sup>38,39</sup>. Linking meteorological drivers and hazards would therefore be difficult based on standard climate model projections.

Apart from modelling limitations, climate change studies of landslide hazards often suffer from the limited availability of precisely dated landslide data which are necessary to link actual landslides to individual hydrometeorological events<sup>40</sup>.

To address the issues outlined above, we specifically consider the 2009 landslide event from Austria and study how such an event would unfold under possible future climatic as well as LULC changes. We develop an event storyline approach<sup>41–43</sup> and ask:

- If a 2009-type event, i.e., an event with the same large-scale circulation would occur in a warmer climate, what would be the associated landslide hazard?

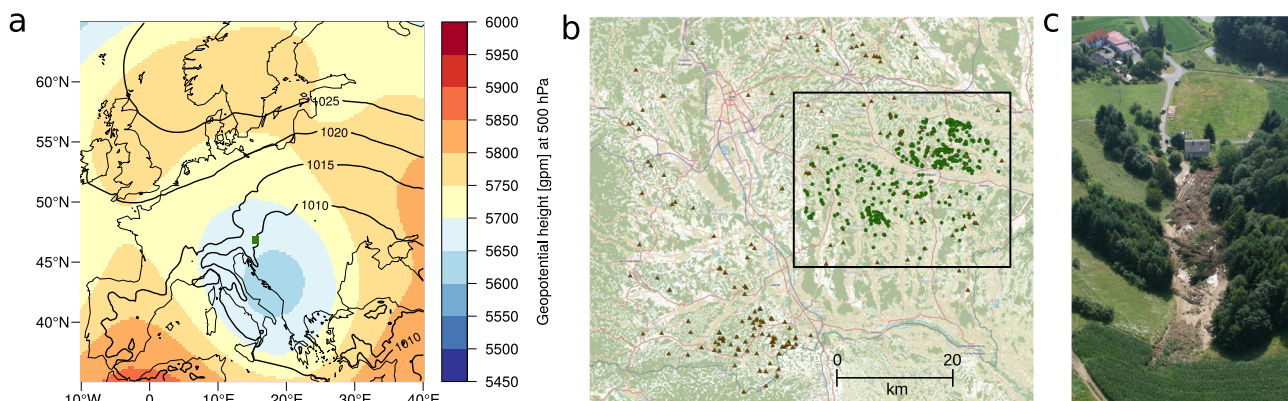


**Fig. 1 Meteorological and landslide event of 2009.** **a** Mean large-scale circulation during 22–26 June 2009 over Europe derived from IFS operational analysis. Sea level pressure (contours, hPa) and geopotential height at 500 hPa (shading, gpm). **b** Map (region marked as green rectangle in **a**) of actual landslides recorded during the 2009 event (green; 2014 landslides additionally used to calibrate the landslide model are marked in brown. See Methods for detail). The target region (roughly coinciding with the Feldbach district and referred to as Feldbach region in the following) considered for the landslide assessment is shown as black rectangle (Supplementary Fig. 1). Map © OpenStreetMap contributors. **c** Aerial view of a landslide occurring during the event. Credit: State of Styria.

- What is the relative contribution of changes in rainfall and soil moisture to changes in the landslide hazard?
- How much would this hazard be reduced if the international community accomplished the Paris agreement?
- How could adaptation by LULC management towards a climate-resilient forest reduce the hazard?

While the main intention of this study is to answer these research questions, it also serves to introduce advances in modelling event storylines, and to demonstrate the power of the overall approach. We find that a substantial increase of landslide hazard from a 2009-type event is plausible in a warmer climate. Without further efforts to reduce greenhouse gas emissions, growth in the area affected by a high landslide occurrence probability of up to 45% has to be considered in climate risk assessments. However, due to substantial uncertainties in rainfall and soil moisture projections, also a reduction of this area should be considered plausible. A successful implementation of the Paris agreement, i.e., limiting global warming to about 0.5 K compared to the present climate, would drastically limit the increase in the affected area from a 2009-type event. Anticipated changes in LULC towards slight afforestation and a climate-resilient forest would help to reduce the affected area and fully compensate for the impacts of warming under the Paris agreement.

## Results

To address the considered research questions, we applied an event storyline approach<sup>41,43</sup>. Such approaches are more and more considered an alternative to classical climate projections for representing climate change uncertainties and assessing climate risk. In our context, the idea is to first simulate the meteorological and landslide event as it happened, and then simulate the event under varying conditions—the storylines—representing a range of possible regional climatic changes and different LULC change scenarios. Here, we briefly sketch the approach. For further details on the approach and information on the data used, please refer to the methods section.

We simulate the 2009 meteorological event as it happened with the high-resolution convection permitting regional climate model (RCM) CCLM<sup>44</sup> over the eastern Alps, using boundary conditions from reanalysis data. This simulation provides a physically consistent evolution of the meteorological conditions, closely resembling the observed weather during the event (Supplementary Fig. 7, Fig. 2).

As landslide hazard, we consider the landslide occurrence probability in a specific location during a 2009-type event. We do not analyse the magnitude and spatial extent of individual landslides. The occurrence probability is assessed with a nonlinear generalised additive model<sup>45</sup>. This statistical landslide model is a modified version of that presented in detail by Knevels et al.<sup>27</sup> and links the landslide occurrence probability to a range of predictors representing geology, topography, LULC, rainfall characteristics and soil moisture prior to the event. The model was calibrated to observed landslides and predictors from the 2009 event and a similar event in 2014.

To assess the future landslide occurrence probability during a 2009-type event, we first simulate a range of hydrometeorological storylines with CCLM, each representing physically consistent and plausible regional climatic changes and thereby sampling climate model uncertainties. In addition, we consider different global warming levels compared to present climate (i.e. the 2009 event): 4 K warming compared to present climate, representing a worst-case scenario; 3 K warming, which is consistent with a business-as-usual scenario; and 0.5 K, which is approximately the amount of warming admissible to still meet the target set in the Paris agreement. Future hydrometeorological predictors for the landslide model are derived from the observed predictor field, modified by predictor-specific change factors<sup>46</sup> calculated from the RCM simulations. We additionally study the sensitivity of the landslide occurrence probability to changing LULC by modifying the corresponding predictors according to several LULC change scenarios. We limit ourselves to changes from agricultural land to forest; all other anthropogenic changes are expected to be relatively minor for the considered region and assumed constant (see Methods section).

To account for possible changes in the large-scale circulation, we complement the storyline approach by an assessment of changes in the types of storms causing rainfall events similar to the 2009 event.

**The event as it happened.** The rainfall event causing the considered landslide event from 2009 was severe across Eastern Austria, but not exceptional. In the Northeast, the 48h rainfall sums correspond to a 50 year event<sup>11</sup>. The severity of the landslide event resulted from the compounding effect of pre-moistening over the preceding winter and spring, and heavy rainfall triggering the actual landslides. The compound character

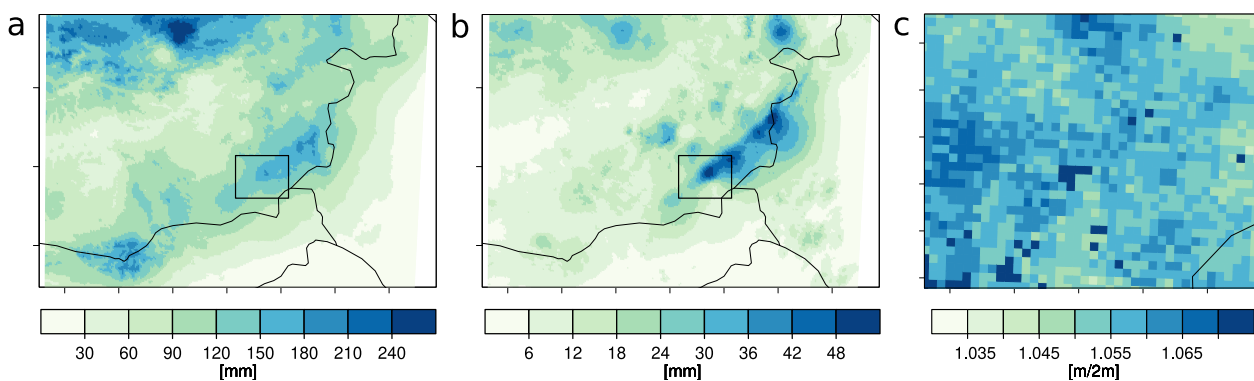


**Fig. 2 Actual rainfall and preconditioning soil moisture over the South-Eastern Alpine forelands.** **a** Maximum 5-day aggregated rainfall ending between 22 and 26 June 2009, and **b** maximum 3-h rainfall between 22 and 26 June 2009 recorded in the INCA data set<sup>64</sup>. **c** Hindcast simulation of maximum 2 m-integrated soil moisture on the day prior to the beginning of the corresponding 5-day rainfall aggregation period. Occurrence dates and thus time periods are chosen individually for each grid box (see Methods for the exact trigger definition for calibrating the statistical model using the landslide dates, which can only be derived for locations where landslides have occurred and thus differ slightly from the definition used for these maps). All panels display the domains used to calculate the delta change factors for the corresponding predictor (13.82E–17.31E and 46.16N–48.01N for precipitation; the target region for soil moisture, marked by the black box in **a**, **b**, see also Supplementary Fig. 1).

of the event is demonstrated by the identified landslide predictors, including 5-day aggregated rainfall prior to the landslide occurrence, the highest 3-h rainfall intensity on the occurrence day, and 2 m aggregated soil moisture prior to the precipitation aggregation period (Fig. 2).

During the event, about 3000 deep and shallow landslides have been recorded in the Feldbach district<sup>10</sup>, their locations mostly coinciding with the high rainfall intensities (Figs. 1 and 2). The predicted landslide occurrence probability (Supplementary Fig. 6) illustrates the influence of high-intensity rainfall, but also clearly indicates the role of topography. Also, LULC was an important determinant of landslide occurrence during the event (Supplementary Figs. 3 and 5): the highest occurrence probability results for areas without forest, whereas it is substantially lower for coniferous forest and even lower for mixed- and broadleaf forest.

**Hydrometeorological storylines.** We represent uncertainties in the regional climate change response by four physical storylines. These storylines describe plausible and physically consistent future unfoldings of the hydrometeorological conditions in a 2009-type event, as simulated by the convection-permitting RCM with changes in the boundary conditions prescribed from four different GCM simulations (Fig. 3 and Table 1).

Five-day aggregated rainfall (left panel) could increase approximately at the Clausius–Clapeyron rate (7%/K; “much heavier rain”; “much heavier rain, drier soil” storylines; see Table 1; note that the scaling here is given with respect to global mean temperature changes, which is in general not identical to the local temperature changes), as is often assumed for extreme precipitation<sup>47</sup>, but also a moderate increase only (“heavier rain, much drier soil”) as well as essentially unchanged conditions (“drier soil”) are plausible. Heavy summer downpours, represented by 3 h maximum rainfall intensities could increase by up to twice the Clausius–Clapeyron rate (10%/K–14%/K; “much heavier rain”; “much heavier rain, drier soil”; “heavier rain, much drier soil” storylines), consistent with other findings on short-term summer extreme rainfall scaling for the region<sup>48</sup>. Again, a zero-change is also possible (“drier soil”). Soil moisture changes range from a strong decrease (“heavier rain, much drier soil”) to a moderate decrease (“much heavier rain, drier soil”; “drier soil”) to essentially constant conditions (“much heavier rain”). The nonlinear response of soil moisture to global warming in the “heavier rain, much drier soil” storyline has not been further investigated, but may be explained with a non-proportional climate change response of the preconditioning precipitation and evapotranspiration. If the target set in the Paris agreement was

accomplished (0.5 K warming), the hydrometeorological changes to the event would be marginal.

**Landslide storylines.** If the 2009 event were to happen in a warmer climate, the landslide occurrence probability could change markedly (Fig. 4). Given the range of possible hydrometeorological changes, also changes in landslide occurrence probability are afflicted with considerable uncertainty. If rainfall intensities were to increase strongly without a substantial decrease in soil moisture (“much heavier rain” and “much heavier rain, drier soil” storylines), the landslide occurrence probability would increase severely. In the core area of the rainfall event, the corresponding odds (see Methods for a definition) would increase by more than 66% in a 4 K warmer world.

But if strong increases in rainfall were compensated by a substantial decrease in soil moisture (“heavier rain, much drier soil” storyline), the odds could even decrease by more than 20% under a 3 K warming. In a 4 K warmer world, the lower soil moisture reduction would be roughly balanced by the rainfall increase; the odds would slightly increase in the core area of the event, but decrease outside. If rainfall were to stay roughly at present-day levels, but with a reduction in soil moisture, the odds would decrease by slightly more than 20% in a warmer world (“drier soil” storyline). For all storylines, accomplishing the goals of the Paris agreement would drastically limit any climate-driven changes in landslide occurrence probability.

Figure 5 summarises the storylines for the area affected by a high landslide occurrence probability resulting from a 2009-type event (see caption for definition). In the worst case (“much heavier rain” and “much heavier rain, drier soil” storylines), this area would increase by about 45% in a 4 K warmer world. In the best case, this area would decrease by about 28% in a 4 K warmer world (“drier soil” storyline) or even 37% in a 3 K warmer world (“heavier rain, much drier soil” storyline). Under the Paris agreement, the area affected by a high landslide occurrence probability during the 2009 event would increase by less than 10%.

The previous results are based on the assumption that landslide occurrence probability does not further increase in response to 5-day aggregated rainfall beyond a threshold of roughly 80 mm. This behaviour is physically plausible and consistent with observational evidence, but we cannot rule out a slight increase of occurrence probability for higher values of 5-day aggregated rainfall. The uncertainty in occurrence probability changes associated with this model uncertainty is, however, only minor. For the “much heavier rain” and “much heavier rain, drier soil”

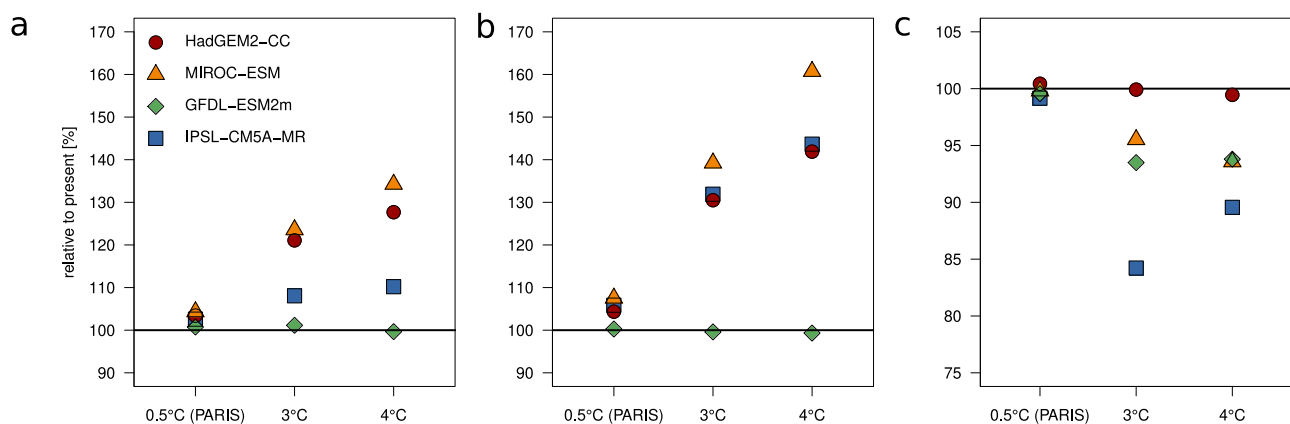


**Fig. 3** Storylines of area-mean rainfall and soil moisture changes. **a** Maximum 5-day rainfall, **b** maximum 3-h rainfall, **c** 2m-integrated soil moisture for different model simulations and warming levels.



**Table 1 Hydrometeorological storylines. Soil moisture values refer to the day prior to the 5-day aggregation period.**

Model	5-day rain	3-h rain	Soil moisture	Description
HadGEM2-CC	++	++	o	much heavier rain
MIROC-ESM	++	++	-	much heavier rain, drier soil
IPSL-CM5A-MR	+	++	--	heavier rain, much drier soil
GFDL-ESM2m	o	o	-	drier soil

++ strong increase, + increase, o no change, - decrease, -- strong decrease.

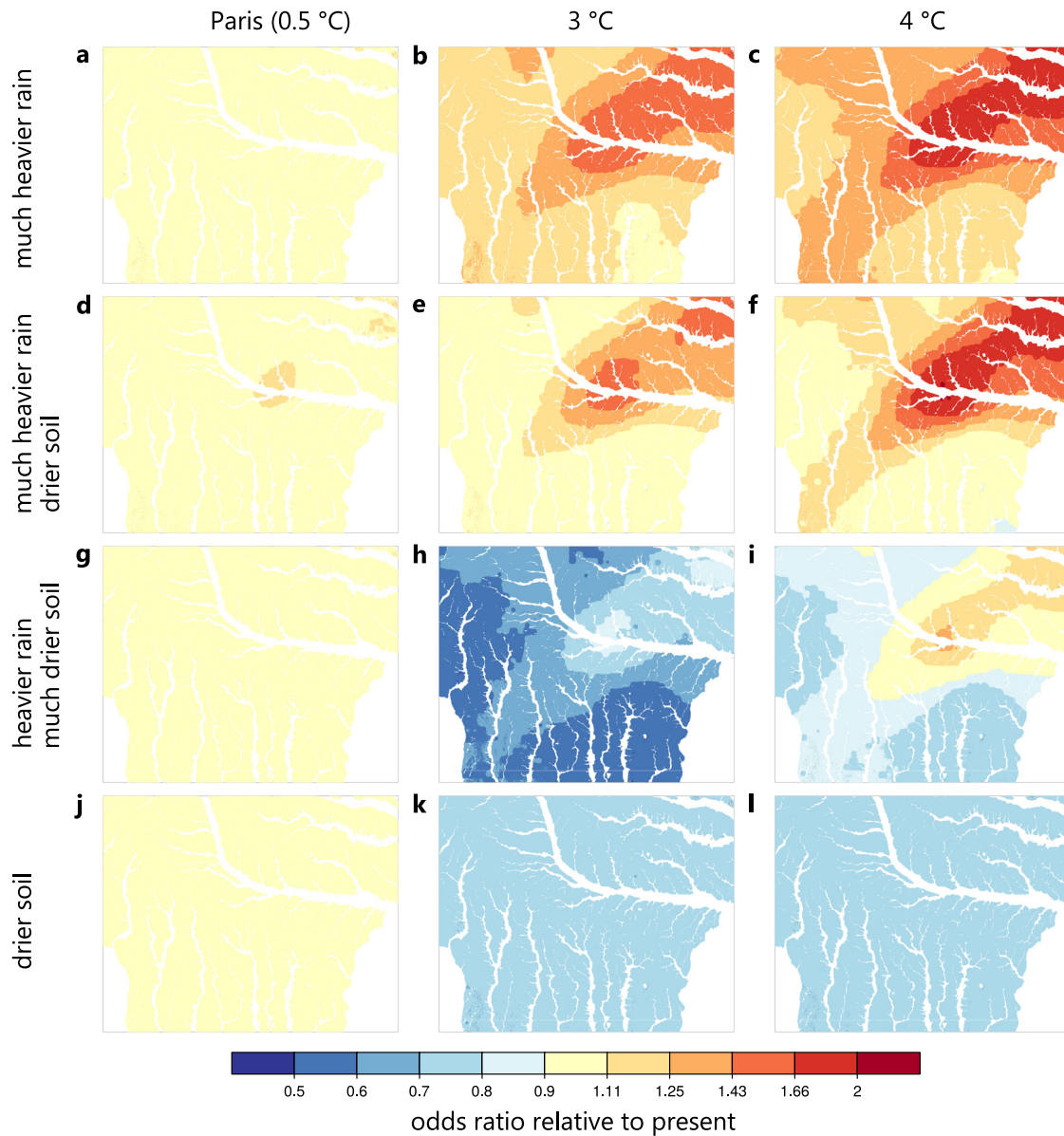


**Fig. 4 Maps of landslide storylines over the Feldbach region.** Odds ratios of landslide occurrence probability during the 2009 event happening in a warmer climate relative to present climate, according to Paris agreement (0.5K warming, left), 3 K warming (middle) and 4 K warming (right). Different storylines from top to bottom: “much heavier rain” (a-c); “much heavier rain, drier soil” (d-f); “heavier rain, much drier soil” (g-i); “drier soil” (j-l).

storylines, such an increase would amplify occurrence probability changes with global warming in the core area of the event by less than about 10% (see Methods for a discussion).

LULC is anticipated to change in the Feldbach region. The agricultural land area is expected to decline in the coming decades as a result of mechanisation, demographic changes and in response to the warming climate. Furthermore, the forestry sector

may adapt to climate change by replacing spruce trees with their shallow root system by climate resilient mixed-leaf forests with typically deeper root systems<sup>49</sup>. We have therefore developed a future LULC scenario in collaboration with local authorities, representing a slight decrease in agricultural land area and proactive forest management towards a climate resilient mixed-leaf forest (Methods). We consider this scenario to represent a

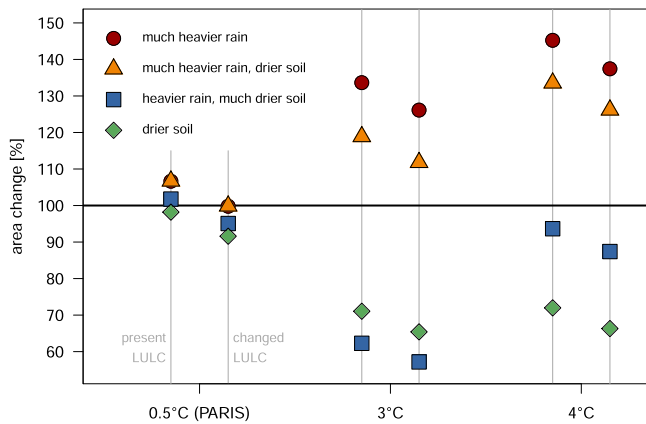


**Fig. 5** Storylines of affected area in the Feldbach region. Change in the area affected by a high landslide occurrence probability of at least 68% within a 10 m × 10 m cell (corresponding to the 95th percentile of landslide occurrence probability across all cells in the Feldbach region in present climate) during the 2009 event happening in a warmer climate. The horizontal black line indicates the present-day reference. For each global warming level, the left symbol shows changes under present-day LULC conditions, the right symbol changes under a climate change resilient forest.

realistic future land cover. These anticipated changes in LULC would help to reduce the landslide occurrence probability compared to storylines with unchanged LULC conditions (Fig. 5). In the worst-case storyline and for a 4 K warming, the growth in area affected by a high occurrence probability would shrink from about 45 to 37%. If the Paris target was met, these land cover changes would fully compensate for the effect of climate change. To further study the possible influence of land cover changes, we additionally considered two idealised scenarios (Supplementary Fig. 8). These scenarios are by no means realistic, but serve to illustrate the role of LULC changes relative to climatic changes. Complete deforestation would dramatically increase the landslide occurrence probability, more than twice as much as for a 4 K warming under present LULC conditions. Conversely, complete afforestation of susceptible land would reduce the area affected by a high landslide occurrence probability to <40% of the present-day area, even in a 4 K warmer world. The effect of such drastic forest cover changes is also much larger than climate model uncertainty (given by the spread across the different storylines).

**Atmospheric circulation changes.** Our storyline approach considers the effect of climate change on landslides given a certain situation of the large-scale atmospheric circulation, i.e. a quasi-stationary storm associated with a cut-off low over the Adriatic sea. If the occurrence probability of the atmospheric circulation pattern would change strongly in a warmer climate, the isolated consideration of the event storyline could be misleading<sup>50</sup>. We, therefore, did not only consider the conditional storylines of the event itself, but also possible changes in the conditioning circulation events.

Unfortunately, to our knowledge no projections of future cut-off low conditions exist so far. But cut-off lows tend to develop as part of atmospheric blocking events<sup>51</sup>, i.e. quasi-stationary anticyclones blocking the mid-latitude westerly flow. Therefore, we consider changes in blocking as a plausible proxy for changes in cut-off lows. Indeed, the June 2009 event was associated with an extensive block, indicated by the high sea-level pressure over eastern Europe (Fig. 1a). European summer blocking, occurring on about 8 days per summer in current climate<sup>52</sup>, is on average projected to decrease, independently of the chosen model

ensembles<sup>52</sup>, and of the exact definition of blocking<sup>53</sup>. Rescaling the results from ref. 52, we find that the frequency of blocked days over Eastern Europe in the CMIP6 models decreases in more than 80% of the individual models, with a mean trend of ~−4% per degree of global mean warming<sup>52</sup>.

In addition to cut-off lows, long-lasting heavy rainfall events in South–Eastern Austria may be caused by Genoa lows<sup>17,18</sup>. Apart from single model studies, changes in Genoa lows in summer have not yet been studied systematically. We, therefore, conducted our own analysis based on a cyclone database from the CMIP5 ensemble in summer<sup>54,55</sup>. For the high-emission RCP8.5 scenario, the frequency of Genoa lows propagating northward towards Central Europe decreases on average by ~−3.3%/K, though only 60% of models agree on a future reduction, partly reflecting large internal climate variability. Quasi-stationary Genoa lows decrease on average at −2.1%/K with 68% of the models showing a decrease. These results suggest a moderate reduction in the occurrence of 2009-type events.

## Discussion

In this study, we develop and apply an event storyline approach to study how a severe landslide event in South–Eastern Austria may unfold under future climate and land-use changes. This approach has proven particularly powerful in our context: It enables us to fully exploit a well-dated landslide data set, with a huge number of events occurring within a couple of days from June 22–26, 2009<sup>56,57</sup>. The approach separates the regional, mostly thermodynamic, climate change response from the “background” state of the large-scale atmospheric circulation<sup>41</sup>. In doing so, we can simulate the event itself without biases in the large-scale circulation, typically arising in transient climate model simulations<sup>54</sup>. Moreover, this separation allows us to use different tailored modelling approaches for the large- and small-scale response. Crucially, focussing on a single event of a few days length allows us to conduct regional climate simulations at a very high resolution and thus to more realistically simulate extreme (and typically convective) summertime rainfall<sup>36</sup>, and to plausibly represent changes in sub-daily rainfall intensities for a range of regional climate change storylines. The storyline approach also aids the communication of climate risk. Choosing the severe 2009 event as an example, we directly connect to the episodic memory of the affected people, helping them to better anticipate future climate risk<sup>41,58</sup>. Our results thereby also provide a familiar event-based frame for regional decision makers<sup>59</sup> to take the hazard from climate change into account, and to raise risk awareness of the general public.

The three most relevant sources of uncertainty in our analysis are uncertainties about the regional response of the climate system to global warming; structural uncertainty of the statistical landslide model under extrapolation to higher rainfall intensities; and the limitation of the considered LULC changes to four vegetation types only. Uncertainty in the regional climate response is explicitly sampled by the four different storylines, i.e., by considering four different GCMs. Structural uncertainty of the landslide model pertains to the inclusion of all relevant predictors and the transformation function between predictors and predictands. Having included preconditioning soil moisture conditions, 5-day aggregated rainfall, and 3-h maximum rainfall, we are confident that all relevant predictors are included. Uncertainties about the transformation function have been estimated for extrapolation of the 5-day aggregated rainfall. Regarding LULC changes, the storyline approach allows for an analysis conditional on non-modelled factors such as the influence of steep or unsecured embankments, filling of slopes and paved areas. We consider these factors as given, and address the additional changes in

hazard due to climatic and forest cover changes. For a detailed discussion of these uncertainties, please refer to the Methods section.

Even though our results strictly apply only for the considered event, they provide insight into the competing roles of changes in different meteorological drivers and LULC for landslides in general. Substantial uncertainties exist about changes in long-duration and short, intense summer rainfall, as well as in the antecedent soil moisture conditions. If a strong rainfall intensification dominates, the area affected by a high landslide occurrence probability may increase by more than 10% per Kelvin warming. Such a rainfall intensification is indeed plausible<sup>15,60</sup>. But a strong reduction in soil moisture could even reduce the overall landslide hazard. Considering soil moisture is therefore crucial for studying the effect of climate change on the landslide hazard, in particular for events in summer, when soil moisture is projected to decrease in many regions of the world<sup>61</sup>. The possibility of a strong increase in landslide occurrence probability should be considered by regional decision makers in climate risk assessments, for instance to define risk zones for regional planning.

In any case, the study highlights the relevance of climate mitigation, and the co-benefits of proactive LULC management for adapting forests to climate change and for reducing the landslide hazard. Idealised scenarios demonstrate that targeted afforestation measures towards a climate resilient mixed-leaf forest could—at least locally—reduce the landslide hazard from the 2009 event below the present-day level even in a 4 K warmer world. Of course, such adaptation measures have to be considered in a broader context. A large area of the district is currently used for agricultural production and will continue to be so in the future. Also, as with any climate change adaptation measure, landslide protection has to be balanced against the conservation of biodiversity<sup>62</sup>. While forests protect very efficiently against landslides<sup>3</sup>, the conservation or restoration of semi-natural orchard meadows may combine basic protection with a species-rich habitat<sup>63</sup>.

## Methods

**Data.** Apart from soil moisture, we used the same data as in Knevels et al.<sup>27</sup>. Please refer to this publication for further details.

Precipitation data were taken from the INCA (Integrated Nowcasting through Comprehensive Analysis) nowcasting system<sup>64</sup> provided by the Austrian weather service (Zentralanstalt für Meteorologie und Geodynamik) to derive present-day meteorological predictors for the statistical landslide model. The original data are provided on a 1 km × 1 km grid at a 15 min resolution but have been aggregated to hourly resolution.

To derive soil moisture data as predictors for the statistical landslide model, we conducted simulations with the HRLDAS (High-Resolution Land Data Assimilation System)<sup>65</sup> on a 1 km × 1 km grid at 1 h resolution, for the period of 2004–2014. Land surface parameters and soil texture types are obtained from the WRF Noah-LSM. The model was initiated with ERA-Interim data<sup>66</sup>. All forcing data was taken from the INCA data set<sup>64</sup>, except for incoming longwave radiation, which was derived by parameterisation<sup>67</sup>, and surface pressure, obtained by extrapolating ERA5 mean sea level pressure<sup>68</sup> onto the INCA surface height.

Topographical predictors for the statistical landslide model were derived from an airborne, LiDAR-based, high-resolution digital terrain model (HRDTM) with a 1 m × 1 m resolution, provided by the GIS department of Styria (GIS-Steiermark). LULC data were derived from the original airborne LiDAR data as well as RapidEye satellite imagery and classified into four classes: (i) no forest, (ii) broadleaf forest (0–25% conifers), (iii) mixed-leaf forest (25–75% conifers), and (iv) coniferous forest (75–100% conifers). All predictors were interpolated to a 10 m × 10 m resolution.

Landslide data for calibrating the statistical landslide model were taken from two events in June 2009 and September 2014. The data were provided by the Institute of Military Geoinformation, the Geological Survey of Austria (2009), and the Styrian Government (2014)<sup>27,56,57</sup>. From all available landslides reported to the authorities, we selected a subset based on minimum size and expert judgement of the data reliability. For the 2009 event, 487 landslides were considered, most of them shallow movements (85%). For the 2014 event, 139 landslides were considered (60% deep-seated, 5% shallow, 35% not classified).

**Land use land cover scenarios.** The government of Styria projects a population decrease of some 10–15% until the year 2060 (no longer projections exist) for the Feldbach region and a strong ageing of the population, while many inhabitants are projected to move towards the city of Graz and its surroundings<sup>69</sup>. We, therefore, expect future changes in the infrastructure and the built environment to be relatively small, and assume that anthropogenic changes are mostly limited to agricultural land use and forests. We thus developed a LULC scenario in collaboration with the Regional Forestry Directorate and the District Forestry Authority. Given that spruce is vulnerable to increasing temperatures and summer dryness<sup>49</sup>, we considered an active forestry management replacing spruce by a climate resilient mixed-leaf forest. Additionally, the land area used for agriculture is expected to decline. We, therefore, defined a LULC scenario by replacing coniferous forest with mixed-leaf forest, and no-forest cover with mixed-leaf forest in areas unfavourable for agriculture (e.g., with steep slopes). Additionally, we considered two idealised scenarios representing extreme de- and afforestation, one where all forest is removed, and one where all no-forest and coniferous forest areas were converted to mixed-leaf forest. The LULC data required to train our landslide model do not allow for further discrimination between different types of non-forested areas.

**Meteorological simulations.** Event storylines have been simulated using the CCLM RCM<sup>44</sup> over the eastern Alpine domain [44.5N–49.1N, 10.7E–19.8E] with 3 km × 3 km grid spacing in convection-permitting mode, i.e. without deep convection parameterisation. For an overview of the chosen model parameterisations see Supplementary Table 1. Soil moisture is explicitly simulated by the RCM land surface component. Boundary conditions for simulating the event as it happened in present climate were taken from the integrated forecast system (IFS) of the European Centre for Medium-Range Weather Forecasts (ECMWF)<sup>70</sup>. The simulation consists of a spin-up from 1 October 2008, 00:00 UTC, to 20 June 2009, 00:00 UTC, to create a balanced soil-moisture field. The spin-up is followed by a ten-member ensemble simulation of the actual event ending at 28 June 2009, 00:00. The different initial conditions are created by staggering the start of the simulations, from 20 June 2009, 00:00 UTC at 3-h intervals backwards in time.

For simulating future storylines, the RCM boundary conditions were altered by changes derived from simulations according to RCP8.5 with four CMIP5<sup>71</sup> GCMs (see Table 1). The changes are designed to represent changes in climate conditions during weather events similar to the 2009 event, and are derived as follows: for the summer months (JJA) of each considered GCM, we calculated the empirical 99th percentile of 3 day aggregated grid-box rainfall over the period 1975–2004 over all grid boxes in the area 13.7E–17.5E and 46N–48N, selected all summer days with events larger than the 99th percentile and calculated mean vertical profiles for these days over the RCM domain of the three-dimensional temperature and relative humidity fields from the surface to the lower stratosphere (35 hPa) as well as sea level pressure. We repeated this analysis for the period 2071–2100 and then calculated differences between the future and present means.

A scaling approach was applied to these composite changes to define different global warming scenarios relative to present climate. To this end, the derived regional temperature, humidity and sea level pressure changes were rescaled with the ratio between the global mean surface temperature change  $\Delta T_{scen}$  for a chosen scenario and the simulated global mean surface temperature change of the chosen GCM simulation (1975–2004 to 2071–2000 under RCP8.5). We chose  $\Delta T_{scen}$  values of 0.5 K (representing the Paris agreement), 3 K (a business-as-usual scenario) and 4 K (a worst-case scenario).

Finally, we applied these composite changes to the IFS data in order to provide modified lateral boundary conditions to the RCM when simulating the event. Thereby, the surface pressure is changed via the changes of sea level pressure taking into account the local orography of IFS. This instantaneously changes the IFS pressure levels. In order to fulfil the hydrostatic equation and to achieve physical consistency, temperature and humidity are adjusted according to the new pressure levels and their vertical extension. Now, the vertical profiles of temperature and humidity changes are added. In the last step, specific humidity is re-calculated from modified temperature, pressure, and relative humidity via the Clausius-Clapeyron relation.

Spin-up simulations to create future soil-moisture fields were conducted in a similar way. Here, the three-dimensional changes in temperature and relative humidity, as well as the changes in sea level pressure, were calculated based on the climatological changes between the present and future period, individually for each day of the year, which were then linearly interpolated in time to provide proper climate change information at each time step during RCM integration in the spin-up period. Thus the future soil moisture predictors represent the expected changes due to changes in rainfall, snow and evapotranspiration during the preceding months.

We selected GCMs spanning a broad range of changes in the selected GCM-simulated rainfall extremes (not shown): IPSL-CM5A-MR, HadGEM2-CC (both with a negative change), GFDL-ESM2m (no change) and MIROC-ESM (strong positive change).

**Delta change approach for the predictors.** The present-day precipitation simulations match very well with observations, but still have slight location biases<sup>72</sup>; soil moisture simulations differ substantially from our reference simulation (supplementary Fig. 7). Moreover, the simulated future precipitation event is



slightly shifted compared to the simulated present-day event (not shown). To overcome these issues and to focus on the thermodynamic component of the change, we therefore do not directly consider the simulated hydrometeorological fields but use these fields to calculate change factors, which are then applied to the observed hydrometeorological fields. In a standard change factor approach<sup>46</sup>, one would calculate long-term differences between the simulated future and present means for a grid box, and add this difference to present day observations. In case of precipitation, ratios are considered instead of differences. As we consider only a single event of a few days length, we cannot reasonably average in time. Instead, we therefore average in space over a region where the climate change signal can be assumed to be constant. Averaging for precipitation is carried out over 13.82E–17.31E and 46.16N–48.01N, which roughly corresponds with the area affected by heavy precipitation during the event. It is large compared to the pattern shifts but small compared to large-scale gradients in the climate change signal. For soil moisture, we average across the actual target domain to avoid an influence of geological variations outside that domain on the climate change signal (note that only one value per day is available for the CCLM soil moisture simulations, but temporal variations are small).

A disadvantage of the standard delta change approach is the fact that it applies an overall change factor across all intensities at all temporal scales. We, therefore, derive change factors separately for all predictors, i.e., 3-h maximum and 5-day aggregated rainfall as well as soil moisture. Change factors are calculated as differences in area averages of present-day and future simulated predictor values. From all permutations of the ten present-day and ten future ensemble members, mean change factors (averaging out the effect of local internal variability) are calculated for the rainfall predictors.

**Statistical landslide modelling.** The landslide occurrence probability is assessed based on a semi-parametric generalised additive model<sup>27,45,73</sup>, which links  $m$  predictors  $x_i$ ,  $i = 1 \dots m$  via transformation functions  $f_i(\cdot)$  and a link function  $g^{-1}(\cdot)$  to the conditional expected value  $E(\cdot)$  of the response, here landslide occurrence probability at a given location,  $Y$ :

$$g(E(Y)) = \beta_0 + f_1(x_1) + \dots + f_m(x_m), \quad (1)$$

The transformation functions can either be parametric (e.g. linear) or non-parametric smoothing functions. The link function is chosen as the logit function  $g(E(Y)) = \log\left(\frac{E(Y)}{1-E(Y)}\right)$ , i.e., the model is a nonlinear logistic regression. The inverse of the logit function maps the predictors onto probabilities (0, 1). The model was calibrated to observed landslides during the 2009 event and a similar, although weaker, event in 2014 in a nearby region (Fig. 1). We found that a model combining shallow and deep-seated landslides performed better and identified physically more plausible predictor–predictand relationships than separate models for the two landslide types<sup>27</sup>. Furthermore, in a model to predict the landslide type, geological predictors had the highest explanatory power, whereas the meteorological predictors during the 2009 and 2014 events could not discriminate between shallow and deep-seated landslides (not shown). We thus decided to use a combined model. More details on the model can be found in Knevels et al.<sup>27</sup>

For our climate change application, we slightly modified the model (Supplementary Figs. 2 and 3): first, we included soil moisture as an additional predictor, to account for a potential soil-drying in a warmer climate. Second, we set the influence of a 5-day aggregated rainfall constant beyond 80 mm (Supplementary Fig. 2). The latter choice was made because the corresponding transformation function was roughly saturated beyond 80 mm, but after a local maximum slightly bending down and then turning upwards again (all within sampling uncertainty). The final upward trend caused a strong increase in landslide occurrence probability with climate change, but we assume that this behaviour was not a physical feature but rather sampling variability (see also discussion below).

The chosen set of predictors comprises geology (five classes: Neogene formations dominated by fine-grained sediments, Neogene formations with coarse-grained layers, pre-Würmian Pleistocene formations, Würmian and Holocene sediments, and other units), land surface variables (convergence index, plan and profile curvature, flow accumulation, normalized height, slope angle, catchment slope, slope aspect, topographic positional index, SAGA wetness index), hydrometeorological variables (5-day aggregated rainfall prior to a landslide in a given  $10 \text{ m} \times 10 \text{ m}$  cell, 3 h maximum rainfall intensity on the day of landslide occurrence in the cell, soil moisture just prior to the 5-day aggregation period), and LULC type (four classes: no forest, mixed-leaf forest, broadleaf, conifer). The transformation functions for the hydrometeorological predictors are shown in Supplementary Fig. 2, the predictive power of the predictors in Supplementary Figs. 3 and 5. To avoid overfitting from predictors explaining only little variability, smoothing penalty terms are integrated that shrink the effect of unimportant predictors to zero<sup>73</sup>. The modified model has been cross-validated as in Knevels et al.<sup>27</sup>. The performance in present climate is essentially identical to that of the model without the soil moisture predictor (Supplementary Fig. 4). Following the reasoning of Maraun and Widmann<sup>46</sup>, we decided to include soil moisture, as, even though it may not have strong predictive power for the 2009 event as it happened, it is an important preconditioning factor and is strongly affected by climate change.

A logistic regression requires observations of events (landslide occurrence) and no-events (no landslide) for calibration. Given that only a small fraction of the district has been screened<sup>27</sup>, the total number of landslides, as well as the total

landslide-free area, are in fact unknown. In cases where the fraction of events is very small compared to the fraction of no-events (as in the case of landslides), an observational sample is therefore typically biased upwards<sup>74</sup>. In such a situation, the predicted landslide occurrence probabilities are too high. In Supplementary Fig. 6 one should thus compare relative values but not interpret absolute values as occurrence probabilities. In Fig. 4, we therefore show odds ratios of future and present landslide occurrence, in Fig. 5 quantiles of the landslide probability distribution across space, which are both unaffected by these biases. The odds associated with a probability  $p$  are defined as  $O = p/(1-p)$ . Odds ratios of future and present landslide occurrence are then defined as the ratio between future and present odds:

$$OR_{fut/pres} = \frac{O_{fut}}{O_{pres}} = \frac{p_{fut}(1-p_{pres})}{p_{pres}(1-p_{fut})}. \quad (2)$$

To understand structural uncertainty in our landslide model, we investigated the plausibility of increasing landslide occurrence probability for 5-day aggregated rainfall above 80 mm. To this end, we considered a linear transformation function, calibrated for all events with 5-day aggregated rainfall above 80 mm. In this case, the landslide occurrence probability would be, compared to the chosen model, <10% higher for the worst-case storyline and a warming of 4 K.

**Cyclone tracking.** Mediterranean extra-tropical cyclones are identified by applying the objective cyclone tracking algorithm TRACK<sup>75</sup> to model output. Cyclones are first identified every 6 h on the 850 hPa vorticity smoothed to T42 resolution by removing the spherical harmonics having total wavenumber <6 and greater than 42. Cyclone tracks are reconstructed by maximising a cost function on track smoothness and speed. The tracks lasting less than two days are discarded. From the resulting cyclone database, two classes of potentially high-impact cyclones, i.e. the quasi-stationary and the Vb-type Genoa lows, are extracted as follows. The quasi-stationary Genoa lows (as the 2009 event) are identified by requiring cyclone genesis in the box (40N–46N, 4E–18E), and at least three days of permanence within the box. The lows following the Vb track are required to have genesis in the same Mediterranean box, but to subsequently pass in Central Europe (47N–55N, 12E–20E) while avoiding the southern Balkans region (38N–45N, 19E–26E)<sup>19</sup>. Finally, both sets of tracks are required an along-track peak intensity based on the 850 hPa smoothed vorticity exceeding  $3 \cdot 10^{-5} \text{ s}^{-1}$ . The methodology is applied to track cyclones in 30-year time slices from the historical (1976–2005) and RCP8.5 (2070–2099) climate simulations of the following 25 CMIP5 climate models: bcc-csm1-1, bcc-csm1-1m, CanESM2, CCSM4, CMCC-CM, CNRM-CM5, CSIRO-Mk3-6-0, EC-EARTH, FGOALS-g2, GFDL-CM3, GFDL-ESM2G, GFDL-ESM2M, HadGEM2-ES, HadGEM2-CC, Inmcm4, IPSL-CM5A-LR, IPSL-CM5A-MR, IPSL-CM5B-LR, MIROC-ESM, MIROC-ESM-CHEM, MIROC5, MPI-ESM-LR, MPI-ESM-MR, MRI-CGCM3, NorESM1-M. The mean projected change is then obtained as follows. First, for each model, cyclone frequency is averaged across all available ensemble members. Then, each model climate change response is obtained as the difference between the RCP8.5 and historical climatologies and scaled by the corresponding increase in the annual-mean global mean surface temperature. Finally, the multi-model mean response is divided by the multi-model mean historical climatology to obtain a percentage change per degree of global-mean warming.

**Applicability of the approach in a climate and LULC change context.** Any statement about future climate change is inherently an extrapolation problem. Confidence about such statements can be gained by comprehensively assessing projection uncertainties, combining multiple sources of information and process understanding<sup>76</sup>. The main climate-change-related uncertainty in our study is climate response uncertainty, i.e., the uncertainty resulting from limitations of climate models in projecting changes of global climate and the regional response to these changes. Climate response uncertainty at the global scale is closely linked to uncertainties about climate sensitivity, i.e., our limited knowledge of how global mean surface temperature responds to CO<sub>2</sub> forcing. By conditioning our results on global warming levels, this uncertainty is (approximately) removed<sup>77</sup>. Regional uncertainties arise both from the GCM-representation of large-scale changes determining the local event, and the RCM-representation of the local event itself. Our storyline approach is particularly powerful to assess these factors. The approach separates the regional, mostly thermodynamic, climate change response from the “background” state of the large-scale atmospheric circulation<sup>41</sup>. In doing so, we can simulate the event itself without biases in the large-scale circulation, typically arising in free-running climate model simulations<sup>54</sup>. This separation furthermore allows us to use different tailored modelling approaches for the large- and small-scale response. On the one hand, we can exploit the full CMIP5 and CMIP6 simulations to assess changes in the atmospheric circulation and their uncertainties. On the other hand, we can conduct regional climate simulations at a very high resolution at a relatively low computational cost. This allows us first to simulate a range of storylines representing local climate response uncertainty resulting from GCM uncertainties, and second to more realistically simulate extreme summertime rainfall<sup>36</sup>, and thus to more plausibly represent changes in sub-daily rainfall intensities for these storylines. All these advantages outweigh the limitation of using one RCM only.



Climate change projections are in general also affected by scenario uncertainty and internal variability<sup>78</sup>. We account for scenario uncertainty—the fundamental inability to predict anthropogenic greenhouse gas emissions into the future—by considering the landslide hazard conditional on different levels of global warming. Furthermore, our event storyline approach allows us to essentially remove uncertainty related to internal variability. The strongest contribution to internal variability usually arises from the large-scale circulation<sup>79</sup>. By keeping the large-scale circulation fixed we remove this source of uncertainty. Additionally, by estimating delta change factors as averages across an ensemble of regional event simulations, we also effectively remove the influence of local-scale internal variability on local changes.

Uncertainties related to the landslide model arise—as in all statistical models applied in a climate change context—from uncertainties about the model structure and parameter uncertainty under extrapolation<sup>46</sup>. Structural uncertainty encompasses whether all predictors controlling the landslide response in a changing climate have been included and whether the predictor–predictand relationship can be extrapolated. The more a statistical model is backed up by physical process understanding, the higher the confidence in the projections<sup>46</sup>. The main factors triggering landslides in our study region are the soil water (both the gravitational effect and the reduction of friction and cohesion) and the mechanical forcing by intense rain<sup>80</sup>. We capture the first factor by the predictors representing soil moisture preconditioning and rainfall, and the second factor by the 3-hour maximum intensity rainfall predictor. To constrain the model as much as possible for extrapolation purposes, we calibrate it to two different events representing two distinct rainfall and soil moisture conditions. A source of structural uncertainty is the influence of 5-day precipitation beyond the observed range. As stated in Section “Statistical landslide modelling”, we compare two models spanning structural uncertainty and estimate the effect on uncertainty in landslide occurrence probability to be less than 10% for a 4 K warming. A final potential source of structural uncertainty is the fact that the statistical model does not discriminate between shallow and deep-seated landslides. But as discussed in Section “Statistical landslide modelling”, a joint model for both types provided physically more plausible results, and meteorological predictors were also not skilful at discriminating between the two types. We are thus confident that uncertainties arising from this issue are of minor importance to our results. Parameter uncertainty of the statistical model arises due to our finite sample. This source of uncertainty will be assessed separately via a bootstrapping approach using a Metropolis–Hastings sampler. It will, however, not qualitatively affect our results.

Also, the results of our LULC change analysis are affected by uncertainties, but again, the storyline approach helps to navigate these<sup>41</sup>. The LULC influence of steep or unsecured embankments, filling of slopes and paved areas on landslide occurrence during the 2009 and 2014 events has not systematically been recorded. Similarly, we also do not have information of the specific agricultural land use prior to the event. These influences therefore cannot be modelled in our statistical approach. In a standard unconditional climate change study, these influences would be confounding factors<sup>42</sup>. But in our storyline approach, we consider these factors as given conditions of the event and address the additional changes in landslide occurrence probability due to climate and LULC change. The decision not to consider changes in the built environment is further justified by the fact that, while the Feldbach region has seen substantial upgrades in the regional infrastructure over recent decades, the state government projects a decrease of the region’s population for the year 2060<sup>69</sup>. We thus expect only relatively minor changes to the area covered by buildings and infrastructure.

## Data availability

IFS boundary conditions for the CCLM RCM can be obtained from the ECMWF (<https://www.ecmwf.int/en/forecasts/datasets/cycle35r2>). ERA5 and ERA-Interim reanalysis data from ECMWF are available from <https://www.ecmwf.int/en/forecasts/datasets/browse-reanalysis-datasets>. Data from the chosen CMIP5 GCM simulations can be downloaded from the Climate and Environmental Retrieval and Archive (CERA) Database (<https://cera-www.dkrz.de/WDCC/ui/cersearch>). Rainfall data from the Integrated Nowcasting through Comprehensive Analysis (INCA) System is available from the Austrian Meteorological Service (<https://data.hub.zamg.ac.at>). Landslide data can be requested from the State of Styria ([rainund.adelwoehrer@stmk.gv.at](mailto:rainund.adelwoehrer@stmk.gv.at)), Geological Survey (GBA, [arben.kociu@geolba.ac.at](mailto:arben.kociu@geolba.ac.at)), and the Institute of Military Geoinformation (IMG, [helene.kautz@bmlv.gv.at](mailto:helene.kautz@bmlv.gv.at)). All topographical predictors are publicly available from GIS-Steiermark (<http://www.gis.steiermark.at>, German only). Source data underlying all manuscript and supplementary figures (apart from Fig. 1b which shows raw landslide locations; this data can be retrieved from the providers listed above) including landslide occurrence probability predictions for all considered storylines can be accessed from <https://doi.org/10.5281/zenodo.6036814>.

## Code availability

Climate simulations were conducted with the community climate model CCLM (<https://wiki.coast.hereon.de/clmcom/>). All statistical modelling and analysis have been conducted in R using the packages `fields` and `mgcv`. The calibrated landslide model as well as custom codes for analysing the landslide predictions including odds ratios and changes in the affected area can be accessed from <https://doi.org/10.5281/zenodo.6036814>. Additional scripts are available upon request.

Received: 30 June 2021; Accepted: 9 March 2022;

Published online: 07 April 2022

## References

1. Jaedicke, C. et al. Identification of landslide hazard and risk ‘hotspots’ in Europe. *Bull. Eng. Geol. Env.* **73**, 325–339 (2014).
2. Crozier, M.J. & Glade, T. In *Landslide Hazard and Risk* (ed. Glade, T) 329–350 (Wiley, 2005).
3. Moos, C. et al. How does forest structure affect root reinforcement and susceptibility to shallow landslides? *Earth Surf. Proc. Land.* **41**, 951–960 (2016).
4. Reichenbach, P., Rossi, M., Malamud, M.D., Mihir, M. & Guzzetti, F. A review of statistically-based landslide susceptibility models. *Earth Sci. Rev.* **180**, 60–91 (2018).
5. Schweigl, J. & J. Hervás. Landslide mapping in Austria. (JRC Scientific and Technical Reports, 2009).
6. Crozier, M.J. Deciphering the effect of climate change on landslide activity: a review. *Geomorphology* **124**, 260–267 (2010).
7. Stefano, L.G. & Guzzetti, F. Landslides in a changing climate. *Earth Sci. Rev.* **162**, 227–252 (2016).
8. Wicki, A. et al. Assessing the potential of soil moisture measurements for regional landslide early warning. *Landslides* **17**, 1–16 (2020).
9. Zscheischler, J. et al. A typology of compound weather and climate events. *Nature Rev. Earth Environ.* **1**, 333–347 (2020).
10. Hornich, R. & Adelwöhrer, R. Landslides in Styria in 2009. *Geomech. Tun.* **3**, 455–461 (2010).
11. Haiden, T. *Meteorologische Analyse des Niederschlags von 22–25*. (Technical report, Zentralanstalt für Meteorologie und Geodynamik, 2009).
12. Jacob, D. et al. EURO-CORDEX: New high-resolution climate change projections for European impact research. *Reg. Environ. Change* **14**, 563–578 (2014).
13. Gobiet, A. & Kotlarski, S. Future Climate Change in the European Alps. *Clim. Sci.* <https://doi.org/10.1093/acrefore/9780190228620.013.767> (2020).
14. Pfahl, S., O’Gorman, P.A. & Fischer, E.M. Understanding the regional pattern of projected future changes in extreme precipitation. *Nat. Clim. Change* **7**, 423–427 (2017).
15. Rajczak, J. & Schär, C. Projections of future precipitation extremes over Europe: a multimodel assessment of climate simulations. *J. Geophys. Res.* **122**, 10–773 (2017).
16. Brönnimann, S. et al. Changing seasonality of moderate and extreme precipitation events in the Alps. *Nat. Haz. Earth Syst. Sci.* **18**, 2047–2056 (2018).
17. Awan, N.K. & Formeyer, H. Cutoff low systems and their relevance to large-scale extreme precipitation in the European Alps. *Theor. Appl. Climatol.* **129**, 149–158 (2017).
18. Hofstätter, M., Lexer, A., Homann, M. & Blöschl, G. Large-scale heavy precipitation over central Europe and the role of atmospheric cyclone track types. *Int. J. Climatol.* **38**, e497–e517 (2018).
19. Nissen, K.M., Ulbrich, U. & Leckebusch, G.C. Vb cyclones and associated rainfall extremes over Central Europe under present day and climate change conditions. *Meteorol. Zeit.* **22**, 649–660 (2013).
20. Volosciuk, C., Maraun, D., Semenov, V.A. & Park, W. Extreme precipitation in an atmosphere general circulation model: impact of horizontal and vertical model resolutions. *J. Climate* **28**, 1184–1205 (2015).
21. Messmer, M.,ómez-Navarro, J.J.G. & Christoph, C.R. Sensitivity experiments on the response of vb cyclones to sea surface temperature and soil moisture changes. *Ear. Syst. Dynam.* **8**, 477–493 (2017).
22. Berg, A., Sheffield, J. & Milly, P.C.D. Divergent surface and total soil moisture projections under global warming. *Geophys. Res. Lett.* **44**, 236–244 (2017).
23. Scheff, J. & Frierson, D.M.W. Scaling potential evapotranspiration with greenhouse warming. *J. Climate* **27**, 1539–1558 (2014).
24. Beniston, M. et al. The European mountain cryosphere: a review of its current state, trends, and future challenges. *Cryosphere* **12**, 759–794 (2018).
25. Glade, T. Landslide occurrence as a response to land use change: a review of evidence from New Zealand. *Catena* **51**, 297–314 (2003).
26. Prommer, C., Puissant, A., Malet, J.-P. & Glade, T. Analysis of land cover changes in the past and the future as contribution to landslide risk scenarios. *Appl. Geogr.* **53**, 11–19 (2014).
27. Knevels, R. et al. Event-based landslide modeling in the Styrian Basin, Austria: accounting for time-varying rainfall and land cover. *Geosciences* **10**, 217 (2020).
28. Ciervo, F., Rianna, G., Mercogliano, P. & Papa, N. Effects of climate change on shallow landslides in a small coastal catchment in Southern Italy. *Landslides* **14**, 1043–1055 (2017).
29. Ciabatta, L. et al. Assessing the impact of climate-change scenarios on landslide occurrence in Umbria region, Italy. *J. Hydrol.* **541**, 285–295 (2016).

30. Gariano, S.L., Rianna, G., Petrucci, O. & Guzzetti, F. Assessing future changes in the occurrence of rainfall-induced landslides at a regional scale. *Sci. Tot. Environ.* **596**, 417–426 (2017).
31. Alvioli, M. et al. Implications of climate change on landslide hazard in Central Italy. *Sci. Tot. Environ.* **630**, 1528–1543 (2018).
32. Peres, D.J. & Cancelliere, A. Modeling impacts of climate change on return period of landslide triggering. *J. Hydrol.* **567**, 420–434 (2018).
33. Parunzio, R. et al. New insights in the relation between climate and slope failures at high-elevation sites. *Theor. Appl. Climatol.* **137**, 1765–1784 (2019).
34. Lin, Q., Wang, Y., Glade, T., Zhang, J. & Zhang, Y. Assessing the spatiotemporal impact of climate change on event rainfall characteristics influencing landslide occurrences based on multiple GCM projections in China. *Clim. Change* **162**, 761–779 (2020).
35. Schlögel, R., Kofler, C., Gariano, S.L., Van Campenhout, J. & Plummer, S. Changes in climate patterns and their association to natural hazard distribution in South Tyrol (Eastern Italian Alps). *Sci. Rep.* **10**, 1–14 (2020).
36. Ban, N. et al. The first multi-model ensemble of regional climate simulations at kilometer-scale resolution, part i: evaluation of precipitation. *Clim. Dyn.* **57**, 1–28 (2021).
37. Kendon, E.J. et al. Do convection-permitting regional climate models improve projections of future precipitation change? *Bull. Amer. Meteorol. Soc.* <https://doi.org/10.1175/BAMS-D-15-0004.1> (2016).
38. Hall, A. Projecting regional change. *Science* **346**, 1461–1462 (2014).
39. Maraun, D. et al. Towards process-informed bias correction of climate change simulations. *Nat. Clim. Change* **7**, 764–773 (2017).
40. van Westen, C.J., van Asch, T.W.J. & Soeters, R. Landslide hazard and risk zonation—why is it still so difficult? *Bull. Eng. Geol. Env.* **65**, 167–184 (2006).
41. Shepherd, T.G. et al. Storylines: An alternative approach to representing uncertainty in physical aspects of climate change. *Clim. Change* **151**, 555–571 (2018).
42. Lloyd, E.A., & Shepherd, T.G. Environmental catastrophes, climate change, and attribution. *Ann. N. Y. Acad. Sci.* <https://doi.org/10.1111/nyas.14308> (2020).
43. Sillmann, J. et al. Event-based storylines to address climate risk. *Earth's Future* **9**, e2020EF001783 (2021).
44. Rockel, B., Will, A. & Hense, A. The regional climate model COSMO-CLM (CCLM). *Meteorol. Z.* **17**, 347–8 (2008).
45. Hastie, T.J. & Tibshirani, R.J. *Generalized Additive Models*. (Chapman & Hall, 1990).
46. Maraun, D. & Widmann, M. *Statistical Downscaling and Bias Correction for Climate Research* (Cambridge University Press, 2018).
47. Allen, M.R. & Ingram, W.J. Constraints on future changes in climate and the hydrological cycle. *Nature* **419**, 2224–2232 (2002).
48. Schroer, K. & Kirchengast, G. Sensitivity of extreme precipitation to temperature: the variability of scaling factors from a regional to local perspective. *Clim. Dynam.* **50**, 3981–3994 (2018).
49. Kolström, M. et al. Reviewing the science and implementation of climate change adaptation measures in European forestry. *Forests* **2**, 961–982 (2011).
50. Otto, F.E.L. et al. The attribution question. *Nat. Clim. Change* **6**, 813–816 (2016).
51. Nieto, R. et al. Interannual variability of cut-off low systems over the European sector: the role of blocking and the Northern Hemisphere circulation modes. *Meteorol. Atmos. Phys.* **96**, 85–101 (2007).
52. Davini, P. & D'Andrea, F. From CMIP3 to CMIP6: Northern Hemisphere atmospheric blocking simulation in present and future climate. *J. Climate* **33**, 10021–10038 (2020).
53. Woollings, T. et al. Blocking and its response to climate change. *Curr. Clim. Change Rep.* **4**, 287–300 (2018).
54. Zappa, G., Shaffrey, L.C. & Hodges, K.I. The ability of CMIP5 models to simulate North Atlantic extratropical cyclones. *J. Climate* **26**, 5379–5396 (2013).
55. Zappa, G., Hawcroft, M.K., Shaffrey, L., Black, E. & Brayshaw, D.J. Extratropical cyclones and the projected decline of winter Mediterranean precipitation in the CMIP5 models. *Clim. Dynam.* **45**, 1727–1738 (2015).
56. Lotter, M., Schwarz, L., Haberler, A. and Kociu, A. Erhebung und Dokumentation gravitativer Massenbewegungen in der Katastrophenregion Feldbach im Sommer 2009. Eine vorläufige Bestandsaufnahme [Survey and documentation of mass movements in the disaster region Feldbach in summer 2009. A preliminary inventory]. Presented at the Landesgeologentag, Graz, Austria, 12 Nov 2009, 2009.
57. Kautz, H. Geodatenaufbereitung in einem Assistenzinsatz des Österreichischen Bundesheeres—am Beispiel Katastrophenregion Feldbach 2009 [Geodata preparation in an assistance mission of the Austrian armed forces—the example of the disaster region Feldbach 2009]. *Proc. Angewandte Geoinformatik* **22**, 638–640 (2010).
58. Schacter, D.L., Addis, D.R. & Buckner, R.L. Remembering the past to imagine the future: the prospective brain. *Nat. Rev. Neurosci.* **8**, 657–661 (2007).
59. Berkhout, F. et al. Framing climate uncertainty: socio-economic and climate scenarios in vulnerability and adaptation assessments. *Reg. Environ. Change* **14**, 879–893 (2014).
60. Pichelli, E. et al. The first multi-model ensemble of regional climate simulations at kilometer-scale resolution part 2: historical and future simulations of precipitation. *Clim. Dyn.* **56**, 3581–3602 (2021).
61. Orlovsky, B. & Seneviratne, S.I. Elusive drought: uncertainty in observed trends and short-and long-term CMIP5 projections. *Hydrol. Earth Syst. Sci.* **17**, 1765–1781 (2013).
62. Pörtner, H.O. et al. Scientific outcome of the IPBES-IPCC co-sponsored workshop on biodiversity and climate change. *IPBES* <https://doi.org/10.5281/zenodo.4659158> (2021).
63. Myczko, L. et al. Effects of management intensity and orchard features on bird communities in winter. *Ecol. Res.* **28**, 503–512 (2013).
64. Haiden, T. et al. The Integrated Nowcasting through Comprehensive Analysis (INCA) system and its validation over the Eastern Alpine region. *Wea. Forecast.* **26**, 166–183 (2011).
65. Chen, F. et al. Description and evaluation of the characteristics of the NCAR high-resolution land data assimilation system. *J. Appl. Meteorol. Climatol.* **46**, 694–713 (2007).
66. Dee, P.D. et al. The ERA-Interim reanalysis: configuration and performance of the data assimilation system. *Quart. J. Royal Meteorol. Soc.* **137**, 553–597 (2011).
67. Gabathuler, M., Marty, A. C. & Hanselmann, K.W. Parameterization of incoming longwave radiation in high-mountain environments. *Phys. Geogr.* **22**, 99–114 (2001).
68. Hersbach, H. et al. The ERA5 global reanalysis. *Quart. J. Roy. Meteorol. Soc.* **146**, 1999–2049 (2020).
69. Abteilung 17 Landes und Regionalentwicklung, Regionale Bevölkerungsprognose. Steiermark—Bundesland, Bezirke und Gemeindegruppen, Heft 3 (2020).
70. Bechtold, P. et al. Advances in simulating atmospheric variability with the ECMWF model: from synoptic to decadal time-scales. *Quart. J. Roy. Meteorol. Soc.* **134**, 1337–1351 (2008).
71. Taylor, K.E., Stouffer, R.J. & Meehl, G.A. *A Summary of the CMIP5 Experiment Design*. [http://cmip-pcmdi.llnl.gov/cmip5/docs/Taylor\\_CMIP5\\_design.pdf](http://cmip-pcmdi.llnl.gov/cmip5/docs/Taylor_CMIP5_design.pdf) (2009).
72. Maraun, D. & Widmann, M. The representation of location by a regional climate model in complex terrain. *Hydrol. Earth Syst. Sci.* **19**, 3449–3456 (2015).
73. Wood, S.N. *Generalized Additive Models: An Introduction With R*. (CRC press, 2017).
74. King, G. & Zeng, L. Logistic regression in rare events data. *Political Anal.* **9**, 137–163 (2001).
75. Hodges, K.I. A general method for tracking analysis and its application to meteorological data. *Mon. Wea. Rev.* **122**, 2573–2586 (1994).
76. Doblas-Reyes, F.J. et al. *Climate Change 2021: The Physical Science Basis. Contribution of Working Group I to the Sixth Assessment Report of the Intergovernmental Panel on Climate Change* (Cambridge University Press, 2021).
77. Chen, D. et al. *Climate Change 2021: The Physical Science Basis. Contribution of Working Group I to the Sixth Assessment Report of the Intergovernmental Panel on Climate Change* (Cambridge University Press, 2021).
78. Stainforth, D.A., Allen, M.R., Tredger, E.R. & Smith, L.A. Confidence, uncertainty and decision-support relevance in climate predictions. *Phil. Trans. R. Soc. A* **365**, 2145–2161 (2007).
79. Shepherd, T.G. Atmospheric circulation as a source of uncertainty in climate change projections. *Nat. Geosci.* **7**, 703–708 (2014).
80. Wieczorek, G. in *Landslides—Investigation and Mitigation* Vol. 247 (eds. Turner, A. K. & Schuster, R. L.) Ch. 4 (National Academy Press, 1996).

## Acknowledgements

This work was funded by the Austrian Climate Research Programme (Projects EASI-CLIM, KR16AC0K13160 and RECLIP CONVEX, KR17AC0K13666) and the Austrian Science Fund (FWF; Research Grant W1256, Doctoral Programme Climate Change: Uncertainties, Thresholds and Coping Strategies). D.M. acknowledges the European COST Action DAMOCLES (CA17109). We thank the Forestry Directorate and the District Forestry Authority for their support in the development of the land cover scenario. We acknowledge computing resources from the Jülich Supercomputing Centre (JSC) and the Vienna Scientific Cluster (VSC) provided via the computing time projects JISC39 and 71193, and the project “GEOCLIM”, funded by the Austrian Federal Ministry of Education, Science and Research, for providing data storage. The IFS data have been provided by the European Centre for Medium-Range Weather Forecasts (ECMWF). The digital elevation model, the geological data and the landslide data from 2014 have been provided by the Federal State of Styria. The landslide data from 2009 have been provided by the Geological Survey of Austria and the Institute of Military Geoinformation. The INCA precipitation data have been made available by the Austrian weather service ZAMG. We thank Ted Shepherd for helpful discussions on the storyline approach.

## Author contributions

D.M. had the idea for the study and designed the overall approach. R.K. calibrated and applied the statistical landslide model with contributions from A.B., H.Pe., H.Pr., P.L.

and D.M. A.N.M., H.T. and E.B. prepared and conducted the RCM simulations. H.Pr. prepared the LULC scenarios with contributions from P.L. G.Z. and B.L.P. performed the cyclone tracking. A.S. conducted soil moisture simulations. D.M., R.K., A.N.M. and G.Z. analysed the results. D.M. wrote the manuscript, with contributions from R.K., A.N.M., H.T., E.B., G.Z., A.B. and A.S. All authors interpreted and discussed the results and commented on the manuscript.

### Competing interests

The authors declare no competing interests.

### Additional information

**Supplementary information** The online version contains supplementary material available at <https://doi.org/10.1038/s43247-022-00408-7>.

**Correspondence** and requests for materials should be addressed to Douglas Maraun.

**Peer review information** *Communications Earth & Environment* thanks Stefan Steger and the other, anonymous, reviewer(s) for their contribution to the peer review of this work. Primary handling editors: Adam Switzer, Heike Langenberg.

**Reprints and permission information** is available at <http://www.nature.com/reprints>

**Publisher's note** Springer Nature remains neutral with regard to jurisdictional claims in published maps and institutional affiliations.



**Open Access** This article is licensed under a Creative Commons Attribution 4.0 International License, which permits use, sharing, adaptation, distribution and reproduction in any medium or format, as long as you give appropriate credit to the original author(s) and the source, provide a link to the Creative Commons license, and indicate if changes were made. The images or other third party material in this article are included in the article's Creative Commons license, unless indicated otherwise in a credit line to the material. If material is not included in the article's Creative Commons license and your intended use is not permitted by statutory regulation or exceeds the permitted use, you will need to obtain permission directly from the copyright holder. To view a copy of this license, visit <http://creativecommons.org/licenses/by/4.0/>.

© The Author(s) 2022